Chapter 12
NSTT and Shooting Method for Periodic Motions

Abstract. In this chapter, two-dimensional shooting diagrams are introduced for visualization of manifolds of periodic solutions and their bifurcations. A general class of nonlinear oscillators under smooth, nonsmooth, and impulsive loadings is considered. The corresponding boundary value problems are formulated by introducing the triangular wave temporal argument. The Duffing oscillator with no linear stiffness (Ueda circuit) is considered for illustration. It is shown that the temporal mode shape of the loading is responsible for qualitative features of the dynamics, such as transitions from regular and random motions. The important role of unstable periodic orbits is discussed.

12.1 Introductory Remarks

Periodic solutions and their bifurcation diagrams often reveal important qualitative features of the dynamics even though the system motion is not expected to be periodic. In particular, the number of periodic orbits, their distribution and properties reveal the structure of chaotic orbits; see, for instance, works [12], [53], [123], and references therein. Direct numerical tools for detection and construction of periodic orbits based on the mapping approach can be found in the book [125] and paper [54]. Different formulations in terms of boundary value problems for ordinary differential equations are described in [10]. Theoretical and applied results regarding periodic motions, bifurcations and chaos are reported in [13] and [196].

In this chapter, a special two-dimensional visualization of the shooting method is introduced in order to incorporate the general two component NSTT as a preliminary analytical stage [144]. Note that the same approach using the one-component NSTT was suggested earlier in [154] and implemented in *Mathematica*® interface [18]. In particular, subharmonic orbits of the forced pendulum and bifurcation diagrams were obtained by examining the shooting curves and their zeros.

V.N. Pilipchuk: Nonlinear Dynamics, LNACM 52, pp. 275–294, 2010.
springerlink.com

Let us consider a multi-dimensional oscillator described be the differential equation

$$F(\ddot{x}, \dot{x}, x, t) = 0 \tag{12.1}$$

where $x(t) \in R^n$, and the vector-function $F \in R^n$ is periodic with respect to time t with the period $T = 4a$.

In this work, different kind of temporal discontinuity in the differential equations of motion will be considered. In order to satisfy the related mathematical requirements, the left-hand side of equation (12.1) must be interpreted in terms distributions [178]

$$\int_{-\infty}^{\infty} F(\ddot{x}, \dot{x}, x, t)\varphi(t)\, dt = 0 \tag{12.2}$$

where $\varphi(t)$ is any sufficiently smooth testing function.

However, at this point, let us assume that the function $F(\ddot{x}, \dot{x}, x, t)$ is regular with no singular terms involved.

Let us consider periodic solutions of the period T by means of the coordinate complexification (NSTT)

$$x \to \{X, Y\}: \qquad x = X(\tau) + Y(\tau)\tau' \tag{12.3}$$

where$\tau = \tau(t/a)$ the triangular sine wave of the period $T = 4a$, and $\tau' = d\tau(t/a)/d(t/a)$ is its first generalized derivative, which is a step-wise discontinuous function at the time instances

$$\Lambda = \{t : \tau(t/a) = \pm 1\} \tag{12.4}$$

As discussed in this book, the above discontinuities can be suppressed by the condition $Y(\pm 1) = 0$, which is the necessary condition of continuity of the original coordinates $x(t)$. Then, assuming for a while no infinite discontinuities in F, substituting (12.3) in (12.1), using the algebraic properties of representation (12.3) as well as other NSTT rules, gives the boundary value problem

$$F\left(\frac{X'' + Y''}{a^2}, \frac{X' + Y'}{a}, \frac{X + Y}{a}, a\tau\right) = 0 \tag{12.5}$$

$$F\left(\frac{X'' - Y''}{a^2}, -\frac{X' - Y'}{a}, \frac{X - Y}{a}, 2a - a\tau\right) = 0 \tag{12.6}$$

$$Y|_{\tau=\pm 1} = 0, \qquad X'|_{\tau=\pm 1} = 0 \tag{12.7}$$

where the prime used with X and Y means differentiation with respect to τ.

Both equations (12.5) and (12.6) are easily derived by the corresponding algebraic manipulations, whereas boundary conditions (12.7) represent the result of elimination of the singular term $\tau''(t/a)$ when substituting (12.3) in

(12.1). In some cases, such a singular term can be employed though in order to eliminate singularities from original equations; see below.

Despite of a relatively complicated form of equations (12.5) and (12.6), the new formulation brings some advantages due to the fact that the new temporal variable τ is bounded and automatically accounts for periodicity of solutions regardless their temporal shapes. This property appears to be important in those cases when the solutions do not represent a final stage of investigation but must be used for further analyses. The dimension increase is often compensated by an effective decrease of the temporal interval of the problem, since the range $-1 \leqslant \tau \leqslant 1$ is covered by the original time domain $-a \leqslant t \leqslant a$, which is twice shorter than the whole period $T = 4a$. Moreover, there are many cases when the number of equations can be reduced to that of the original system due to the symmetry of equations. If, for instance, the vector-function $F(\ddot{x}, \dot{x}, x, t)$ is even with respect to the velocity $\dot{x}$ or includes no velocity at all, and the explicit dependence on time t produces zero 'imaginary component' then boundary value problem (12.5) through (12.7) admits a family of solutions on which

$$Y \equiv 0, \qquad F\left(\frac{X''}{a^2}, \frac{X'}{a}, \frac{X}{a}, a\tau\right) = 0 \tag{12.8}$$

$$X'|_{\tau=\pm 1} = 0 \tag{12.9}$$

The particular case (12.8) and (12.9) was investigated numerically by the shooting method in [154] and [177] based on a single- and multiple-degrees-of freedom systems, respectively. It should be noted that no special requirements are imposed on numerical methods or packages for solving the above boundary-value problems. However, the shooting algorithm in the *Mathematica*® interface provides a physically meaningful way of visualization of periodic solutions due to the specific combination analytical and numerical commands.

12.2 Problem Formulation

Let assume now that the system loading may include a periodic series of Dirac δ-pulses acting at times Λ(12.4). As is known [45], Dirac δ-functions can participate in nonlinear differential equations only as summands because nonlinear manipulations with δ-functions are physically meaningless, except special concepts [106]. Therefore, the original equation (12.1) must be concretized as

$$\ddot{x} + f(x, \dot{x}, t) = q\,(t) \tag{12.10}$$

where

$$q\,(t) = Q\,(\tau\,(t/a)) + P\,(\tau\,(t/a))\,\tau'\,(t/a) + p\,(\tau\,(t/a))\,\tau''\,(t/a) \tag{12.11}$$

and

$$\tau''(t/a) = d^2\tau(t/a)/d(t/a)^2 \tag{12.12}$$
$$= 2\sum_{k=-\infty}^{\infty}\left[\delta\left(\frac{t}{a}+1-4k\right)-\delta\left(\frac{t}{a}-1-4k\right)\right]$$

In equation (12.10), the function $f(x,\dot{x},t)$ may still include parametric terms of the period $T=4a$ with possible step-wise discontinuities on Λ. The acceleration $\ddot{x}$ also participates as a summand, since it must have the same kind of singularities as the external forcing function, $q(t)$. According to the distribution theory [165], $p(\tau(t/a))$ must be at least continuous on Λ, otherwise the 'product' $p(\tau)\tau''$ cannot be treated as a distribution. Note, that behavior of the function $p(\tau(t/a))$ between the times Λ is arbitrary, since only values $p(-1)$ and $p(1)$ contribute into the expression

$$p(\tau(t/a))\tau''(t/a) \tag{12.13}$$
$$= 2\sum_{k=-\infty}^{\infty}\left[p(-1)\delta\left(\frac{t}{a}+1-4k\right)-p(1)\delta\left(\frac{t}{a}-1-4k\right)\right]$$

The numbers $p(-1)$ and $p(1)$ control the 'amplitudes' and directions of the $\delta-$pulses. For example, all the pulses can be positively co-directed by setting $p(\tau) = -\operatorname{sign}\tau$.

Remark 2. Expressions (12.3) and (12.11) represent particular cases of the truncated series

$$q(t) = \sum_{k=0}^{N} P_k(\tau(t/a))\, d^k\tau(t/a)/d(t/a)^k \tag{12.14}$$

where $P_k(\tau(t/a))$ must be at least $k-2$ times continuously differentiable in the neighborhood of points $t=\pm a$. Although, physical interpretation of the higher order terms in (12.14) is not straightforward, such terms still can occur after reducing the number of equations from the entire system. In case (12.10) and (12.11), one has $N=2$ and therefore the velocity vector $\dot{x}$ must be step-wise discontinuous. Further, if $N=3$ then the velocity $\dot{x}$ includes singular terms and the function $f(x,\dot{x},t)$ in equation (12.10) must be linear with respect to $\dot{x}$. If $N=4$ then the function $f(x,\dot{x},t)$ must be linear also with respect to the position vector x provided that any parametric terms are sufficiently smooth functions of time. Therefore, only linear systems can be considered if $N \geq 4$.

Since the basis elements $\{1,\tau',\tau''\}$ represent functions of different classes of smoothness, then substituting (12.3) and (12.11) in (12.10), gives separately

$$a^{-2}X'' + R_f(X,Y,X',Y',\tau) = Q(\tau) \tag{12.15}$$

$$a^{-2}Y'' + I_f\left(X, Y, X', Y', \tau\right) = P\left(\tau\right) \tag{12.16}$$

and

$$a^{-2}X' \mid_{\tau=\pm1} = p\left(\pm1\right) \tag{12.17}$$

where

$$\left\{ \begin{matrix} R_f \\ I_f \end{matrix} \right\} = \frac{1}{2}\left[f\left(X+Y,\ \frac{X'+Y'}{a}, a\tau\right) \pm f\left(X-Y,\ -\frac{X'-Y'}{a}, 2a-a\tau\right)\right] \tag{12.18}$$

Note that the singular term $a^{-1}Y\tau''$ is eliminated from the velocity vector $\dot{x}\left(t\right)$ by imposing another boundary condition

$$Y \mid_{\tau=\pm1} = 0 \tag{12.19}$$

The boundary value problem (12.15) through (12.19) includes no singular or discontinuous functions, therefore standard numerical codes and packages can be applied with no specific constraints on their choice.

In general, equations (12.15) and (12.16) are coupled. Although the equations can be decoupled by introducing the new unknown functions, $X(\tau) + Y(\tau)$ and $X(\tau) - Y(\tau)$, the boundary conditions will become coupled. There are two special cases, however, when the entire problem can be reduced. If, for instance, $f\left(x, \dot{x}, t\right) = f\left(x, -\dot{x}, 2a-t\right)$, and $P\left(\tau\right) \equiv 0$ then the problem admits a family of solutions such that

$$Y \equiv 0, \quad a^{-2}X'' + f\left(X,\ X'/a, a\tau\right) = Q\left(\tau\right) \tag{12.20}$$

under the boundary condition (12.17).

In case $f\left(x, \dot{x}, t\right) = -f\left(-x, \dot{x}, 2a-t\right)$, $Q\left(\tau\right) \equiv 0$ and $p\left(\tau\right) \equiv 0$, then one can consider another family of solutions on which

$$X \equiv 0, \quad a^{-2}Y'' + f\left(Y,\ Y'/a, a\tau\right) = P\left(\tau\right) \tag{12.21}$$

under the boundary condition (12.19).

This chapter nevertheless focuses on the general two-component problem (12.15) through (12.19).

12.3 Sample Problems and Discussion

12.3.1 Smooth Loading

The Duffing-Ueda oscillator [186] under the periodic loading of different temporal shapes will be considered below.

Let us start with the standard case of sine-wave voltage

$$\ddot{x} + \zeta\dot{x} + x^3 = B\sin\omega t \tag{12.22}$$

where ζ, B, and ω are constant parameters.

In this case, the differential equations (12.15) and (12.16) take the form

$$a^{-2}X'' + \zeta a^{-1}Y' + X^3 + 3XY^2 = B\sin\frac{\pi\tau}{2} \tag{12.23}$$

$$a^{-2}Y'' + \zeta a^{-1}X' + Y^3 + 3X^2Y = 0 \tag{12.24}$$

where $a = \pi/(2\omega)$ is a quarter of the loading period, and the boundary conditions are

$$Y\,|_{\tau=\pm1} = 0, \quad X'\,|_{\tau=\pm1} = 0 \tag{12.25}$$

The shooting method can be applied now as follows. First, the differential equations (12.23) and (12.24) are solved under the *initial conditions*

$$X(-1) = g, \quad X'(-1) = 0 \tag{12.26}$$

$$Y(-1) = 0, \quad Y'(-1) = h \tag{12.27}$$

where g and h are numbers to be determined in order to satisfy boundary conditions (12.25).

Let us represent solution of the initial-value problem (12.23), (12.24), (12.26) and (12.27) in the following general form

$$X = X(\tau; g, h), \quad Y = Y(\tau; g, h) \tag{12.28}$$

By the idea of shooting method, the initial value problem (12.23), (12.24), (12.26) and (12.27) must be iteratively solved multiple times at different g and h until sufficient precision has been reached for boundary conditions (12.25) at right end $\tau = 1$,

$$\begin{aligned} \frac{\partial X(\tau; g, h)}{\partial \tau}|_{\tau=1} &\equiv G(g, h) = 0 \\ Y(\tau; g, h)|_{\tau=1} &\equiv H(g, h) = 0 \end{aligned} \tag{12.29}$$

When dealing with the particular cases (12.20) or (12.21), such a procedure is not difficult since one has only one equation with a singe unknown, $G(g) = 0$ or $H(h) = 0$. Multidimensional cases, such as (12.29), appear to be more difficult and time consuming. From this point of view, the important feature of *Mathematica* is that it is possible to program the functions $G(g, h)$ and $H(g, h)$ 'explicitly' in such a way that the arguments g and h are included into the numerical solver of differential equations. This can be done as follows. First, the numerical solution is defined as a function of the arguments g and h according to the command

sol[g_, h_]:=NDSolve[{eqX, eqY,

X[-1]==g, X′[-1] == 0, Y[-1] == 0, Y′[-1] == h}, {X,Y}, {τ,-1,1}];

where eqX and eqY are equations (12.23) and (12.24), respectively.

Then, the functions $G(g,h)$ and $H(g,h)$ are defined as follows

$$\text{G[g\_, h\_]:=X}'\text{[1]/.sol[g, h][[1]];}$$

$$\text{H[g\_, h\_]:=Y[1]/.sol[g, h][[1]];}$$

As a result, the functions $G(g,h)$ and $H(g,h)$ can be considered as usual functions of two arguments. In particular, intersections of two manifolds (12.29) can be located and determined by using the commands *ContourPlot* and *FindRoot,* respectively. Each of the determined roots of equations (12.29) represents a periodic solution of the original equation. If the loading amplitude B is a control parameter, then the evolution of diagrams $G(g,h;B)=0$ and $H(g,h;B)=0$ represents the corresponding structural changes in the set of periodic solutions.

Fig. 12.1 gives an example of such a diagram. The parameters were chosen in order to provide conditions for the 'randomly transitional' process in terms of work [186]. The diagram clearly shows five intersections between the two different families of curves. The corresponding solutions of the input period $T=4a=2\pi$ are shown in Figs. 12.2 and 12.3.

Direct numerical solutions the corresponding estimates for Floquet multipliers show that first four periodic solutions, (a) through (d), are unstable, and only one solution (e) is stable. Solution (e) was detected by direct analog and digital computer simulations reported in [186], whereas solutions (a) through (d) were unlisted. Instead, a 'non-reproducible trajectory' as a realization of the 'randomly transitional' process was represented in the xv-plane. Such a trajectory can be treated as a chaotic drift around the first three unstable motions (a), (b) and (c). However, high order periodic solutions may also affect the dynamics of chaotic drift [12].

Fig. 12.4 shows what actually happens when trying to numerically reproduce an unstable periodic orbit, say (a). Neither the shooting algorithm nor computer codes allow to perfectly introduce the initial conditions, therefore it is unlikely that the oscillator will remain on the unstable orbit. After few cycles, the system leaves the orbit (a) for the 'randomly transitional' drift around the all three unstable orbits (a), (b) and (c) with 'no certain choice' between them. The long-term time history and the corresponding spectrogram of this motion, represented in Fig. 12.4, confirm its random character during quite a long period of time.

Although preliminary qualitative information about stability or instability of periodic solutions can be obtained by direct numerical tests, one can quantify stability properties based on the well known Floquet theory in terms of the characteristic multipliers [111], [56]. In order to remind the principals, let us consider periodic solution $x(t)$ of the equation (12.10),where $f(x,\dot{x},t)=f(x,\dot{x},t+T)$, $q\,(t)=q\,(t+T)$, and the period is $T=4a$.

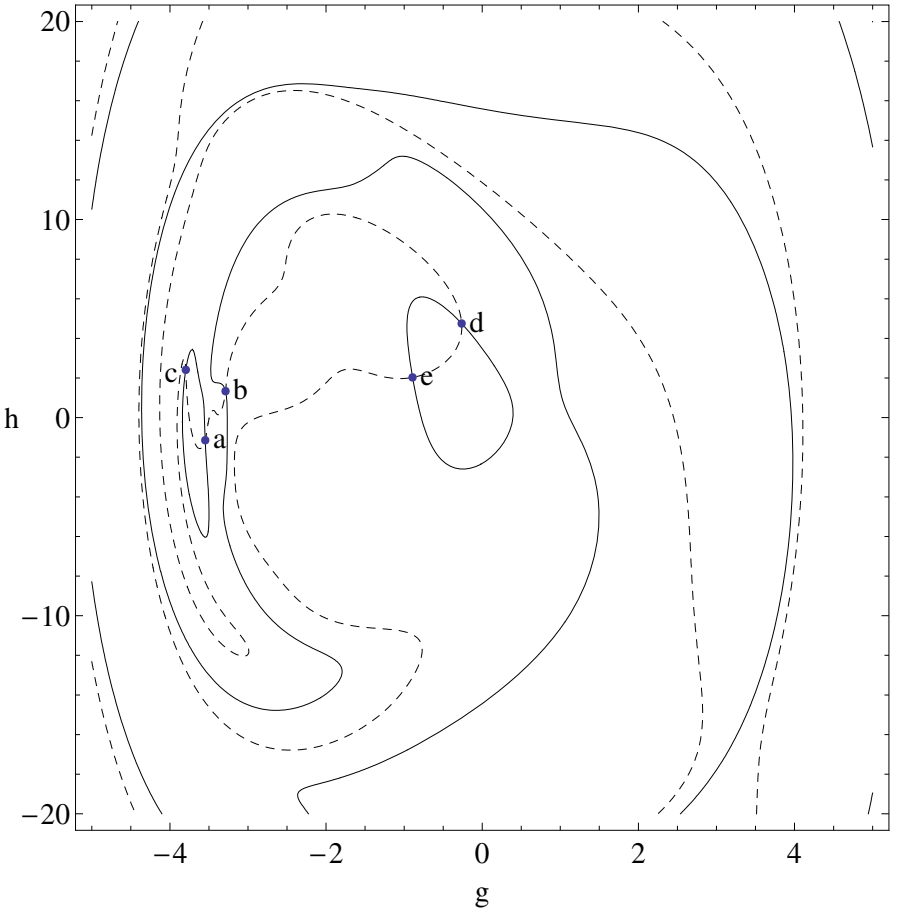

Fig. 12.1 The curves $G(g,h)=0$ (continuous) and $H(g,h)=0$ (dashed) and their intersections for the Ueda oscillator under the sine-wave input and the following parameters: $\zeta=0.1$, $B=12$, and $\omega=1$ (0.1592 Hz).

A variation of the solution $x(t)$, say $u(t)$, is described by the linear differential equation with periodic coefficients

$$\ddot{u}+q_1(t)\dot{u}+q_2(t)u=0$$

where $q_1(t)=\partial f(x,\dot{x},t)/\partial\dot{x}$ is assumed to be independent on $\dot{x}$, and $q_2(t)=\partial f(x,\dot{x},t)/\partial x$.

Then substitution

$$u=y(t)\exp\left(-\frac{1}{2}\int_0^t q_1(z)dz\right)$$

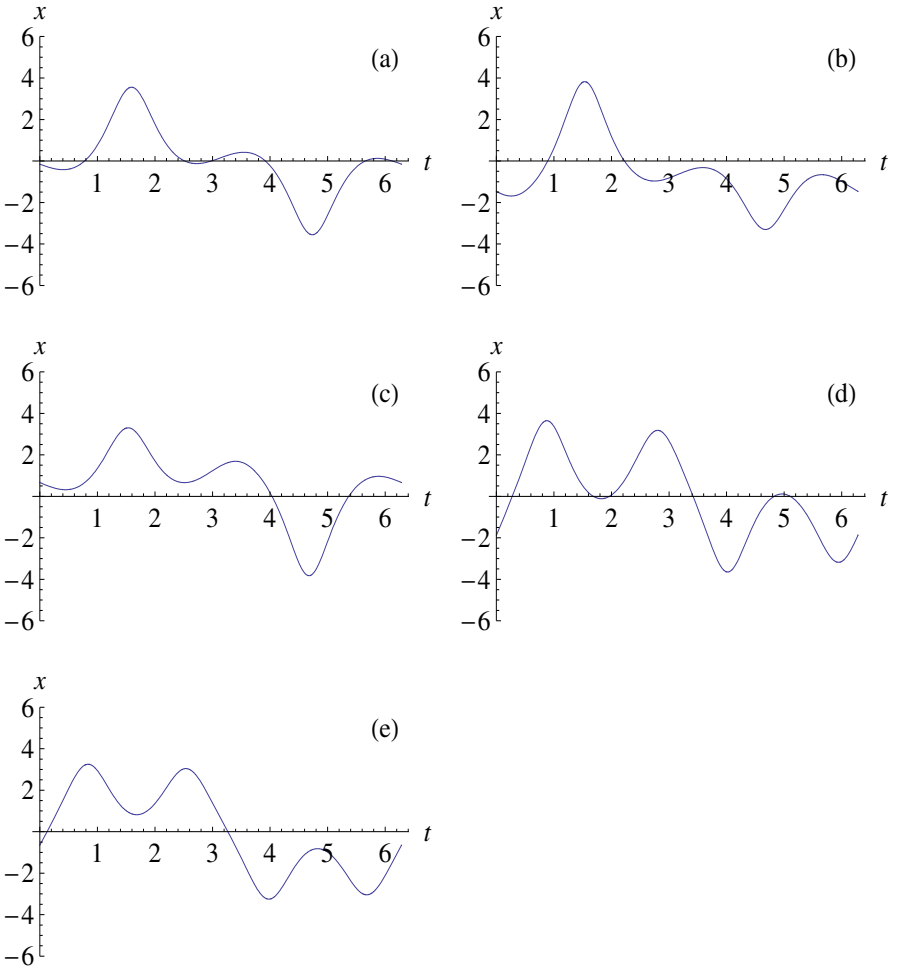

Fig. 12.2 The temporal mode shapes of periodic solutions.

gives

$$\ddot{y} + p(t)y = 0 \tag{12.30}$$

where

$$p(t) = q_2(t) - \frac{1}{4}[q_1(t)]^2 - \frac{1}{2}\dot{q}_1(t)$$

As known from the Floquet theory, stability of the solution $x(t)$ is determined by the Floquet multipliers

$$\mu_{1,2} = A \pm \sqrt{A^2 - 1} \tag{12.31}$$

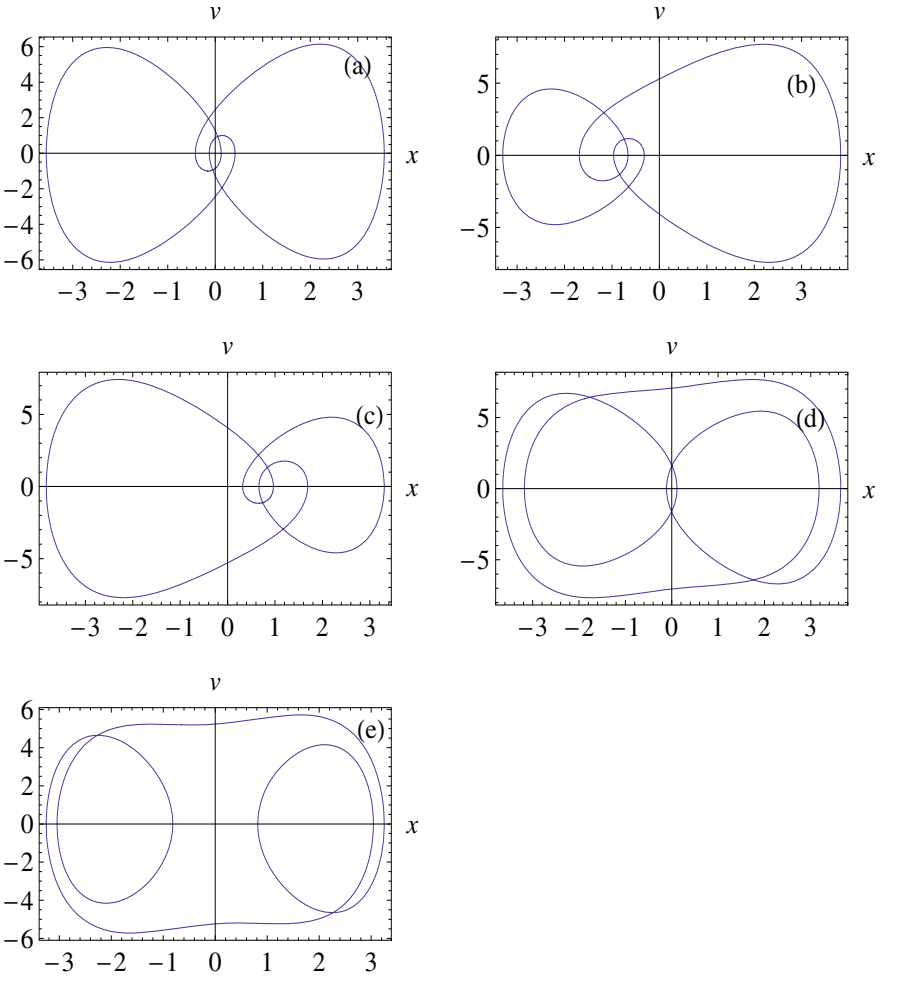

Fig. 12.3 The projections of periodic trajectories on xv-planes.

where $A = [y_1(T) + \dot{y}_2(T)]/2$, and $y_1(t)$ and $y_2(t)$ are two fundamental solutions of equation (12.30) given by the initial conditions

$$y_1(0) = 1, \quad \dot{y}_1(0) = 0$$
$$y_2(0) = 0, \quad \dot{y}_2(0) = 1$$

Based on the number A, the solution $x(t)$ is unstable if $A^2 > 1$, and it is stable if $A^2 < 1$. In case $A^2 = 1$, there exist a periodic solution of equation (12.30).

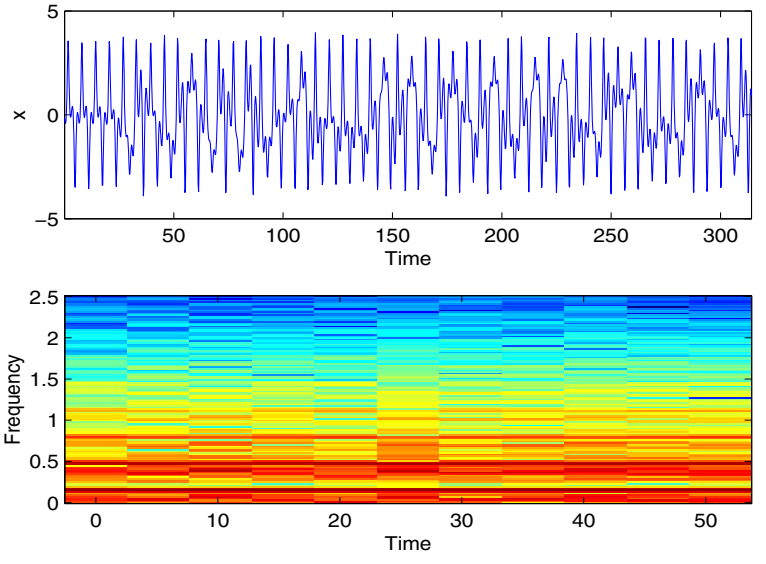

Fig. 12.4 The time history record and its spectrogram (in Hz) for Ueda oscillator after the direct numerical integration. The parameters are: $\zeta = 0.1$ and $B = 12.0$.

Now, let $x(t)$ be a periodic solution of equation (12.22). The corresponding variational equation is

$$\ddot{u} + \zeta\dot{u} + 3x^2u = 0 \tag{12.32}$$

where $u = u(t)$ is a small variation of the solution $x = x(t)$.

After the standard substitution $u(t) = y(t)\exp(-\zeta t/2)$, equation (12.32) takes the form

$$\ddot{y} + \left(3x^2 - \frac{\zeta^2}{4}\right)y = 0$$

Taking into account the form of solution (12.3), gives the variational equation with periodic coefficient

$$\ddot{y} + [U(\tau(t/a)) + V(\tau(t/a))\tau'(t/a)]y = 0 \tag{12.33}$$

where $U(\tau) = 3X^2(\tau) + 3Y^2(\tau) - \zeta^2/4$ and $V(\tau) = 6X(\tau)Y(\tau)$.

Note that the periodic coefficient in equation (12.32) is continuous with respect to time t since $V(\pm 1) = 0$ due to the boundary conditions (12.25).

By using the numerical solutions of equation (12.33), one obtains the number A for every solution

$$A_a = 10.5155,\ A_b = -2.63747,\ A_c = -2.63749$$

$$A_d = 1.70201, \text{ and } A_e = 0.143507 \tag{12.34}$$

where the index correspond to the type of periodic solution of the original equation; see Figs. 12.1, 12.2, and 12.3. These numbers confirm that only solution (e) is stable.

12.3.2 Step-Wise Discontinuous Input

Let us consider now the case of discontinuous periodic input of the rectangular cosine temporal shape

$$\ddot{x} + \zeta\dot{x} + x^3 = B\frac{d\tau\,(t/a)}{d\,(t/a)} \tag{12.35}$$

where a is a quarter of the input period.

In this case, the right-hand side of equations (12.23) and (12.24) are modified so that the equations take the form

$$a^{-2}X'' + \zeta a^{-1}Y' + X^3 + 3XY^2 = 0 \tag{12.36}$$

$$a^{-2}Y'' + \zeta a^{-1}X' + Y^3 + 3X^2Y = B \tag{12.37}$$

under the homogeneous boundary conditions (12.25).

Fig. 12.5 shows the shooting diagram under the fixed parameters $\omega = \pi/(2a) = 1$ (0.1592 Hz), $B = 7.4$ and $\zeta = 0.05$. In this case, there are seven intersections between the two families of curves and therefore seven periodic solutions of the period $T = 4a$ as shown in Figs. 12.6 and 12.7.

Note that, under the same parameters, the system response on the rectangular cosine input shows new features compared to those under the sine-wave input [144]. For example, after few cycles along the orbit (a), the system starts its drift around the first three solutions, (a), (b) and (c). At this stage, the dynamics resembles that under the sine-wave input. Further, however, after several random 'jumps' between the orbits (a), (b) and (c), the system becomes eventually attracted by the stable orbit (e). The direct numerical solution, represented in Fig. 12.8, clearly shows all three stages of the time and spectral histories of the dynamics.

In order to clarify stability, the Floquet theory can be applied analogously to the case of the sine-wave input.

12.3.3 Impulsive Loading

Let us consider the same oscillator loaded by the periodic series of pulses

$$\begin{aligned}\ddot{x} + \zeta\dot{x} + x^3 &= p\tau'' \\ &= 2p\sum_{k=-\infty}^{\infty}\left[\delta\left(\frac{t}{a} + 1 - 4k\right) - \delta\left(\frac{t}{a} - 1 - 4k\right)\right]\end{aligned} \tag{12.38}$$

where $p = p\,(\pm 1) = B = const.$

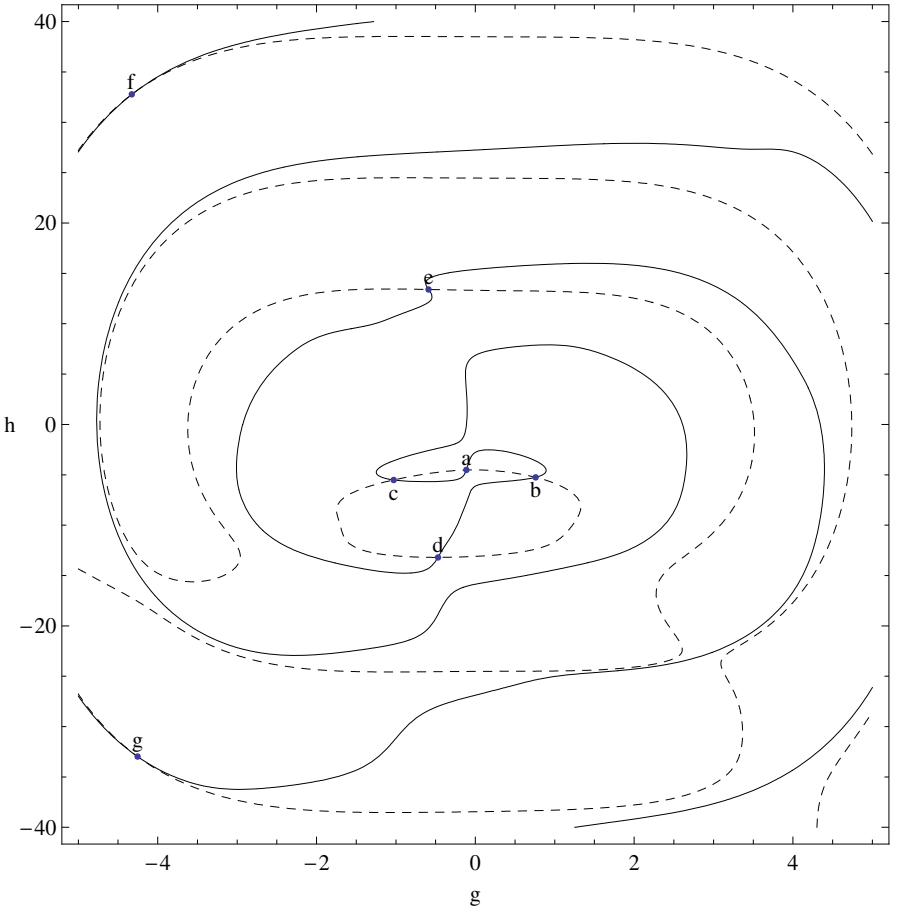

Fig. 12.5 The curves $G(g,h) = 0$ (continuous) and $H(g,h) = 0$ (dashed) for the Ueda oscillator under the step-wise input and the following parameters: $\zeta = 0.05$, $B = 7.4$, and $\omega = 1$.

In this case, both equations (12.36) and (12.37) should have zero right-hand side, however, the non-homogeneous version of the boundary condition (12.17) must be imposed in order to eliminate the pulses. The second expression in (12.26) and the first one in (12.29) must be modified as $X'\ (-1)\ = a^2 B = [\pi/(2\omega)]^2 B$ and $G\,(g,h) = a^2 B = [\pi/(2\omega)]^2 B$, respectively. Therefore, the singular terms are eliminated from the system due to the saw-tooth time, and the shooting procedure can be applied in the same fashion as that under the smooth input. The shooting diagram and the corresponding periodic solutions are shown in Figures 12.9, and 12.10 and 12.11, respectively.

The projections of the phase trajectories show discontinuities of the velocity on the xv-plane caused by the external pulses. The last four projections,

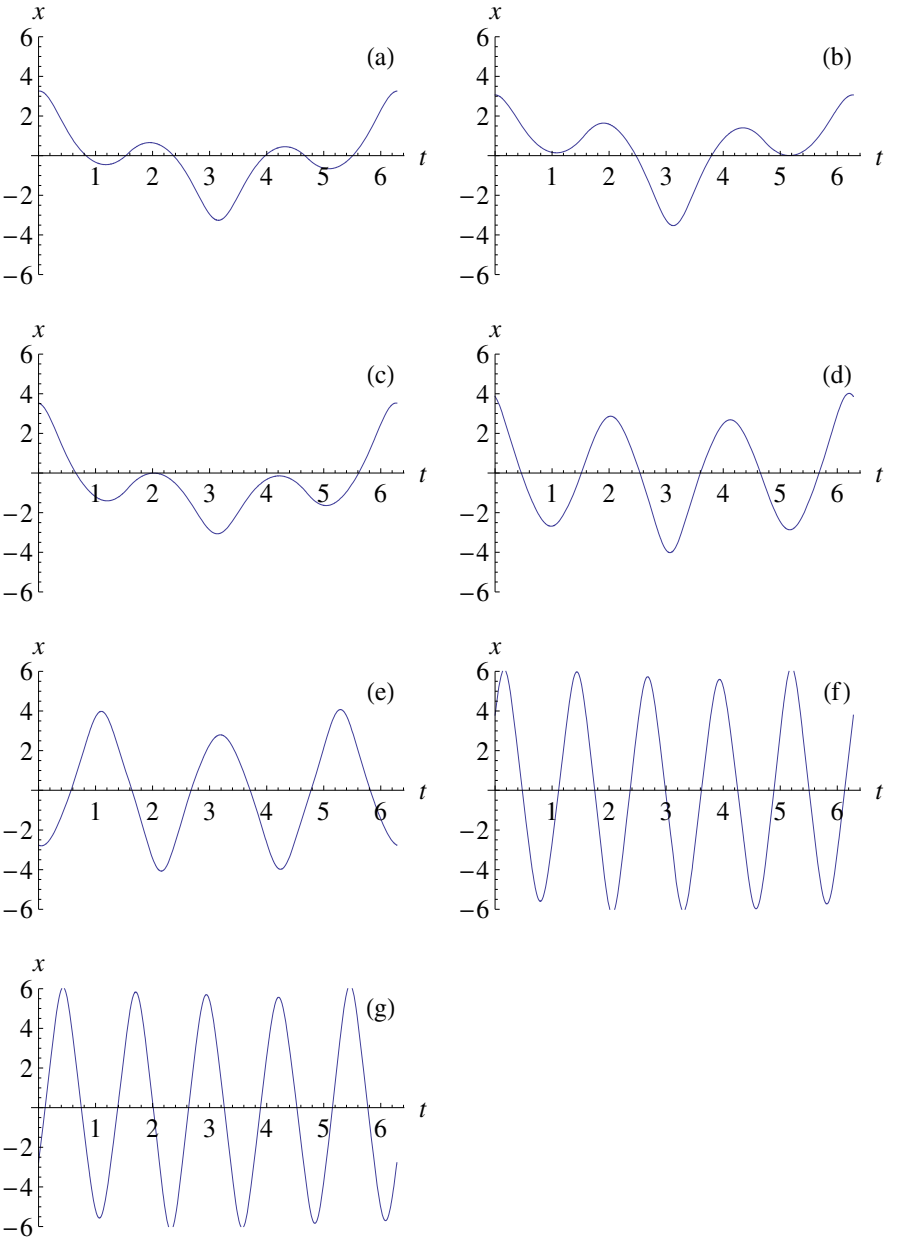

Fig. 12.6 The temporal mode shapes of periodic solutions og Ueda circuit under the step-wise input.

(h) through (k), can be qualified as 'quasi free' vibrations sustained by the pulses. In the shooting diagram represented in Fig. 12.9, the related

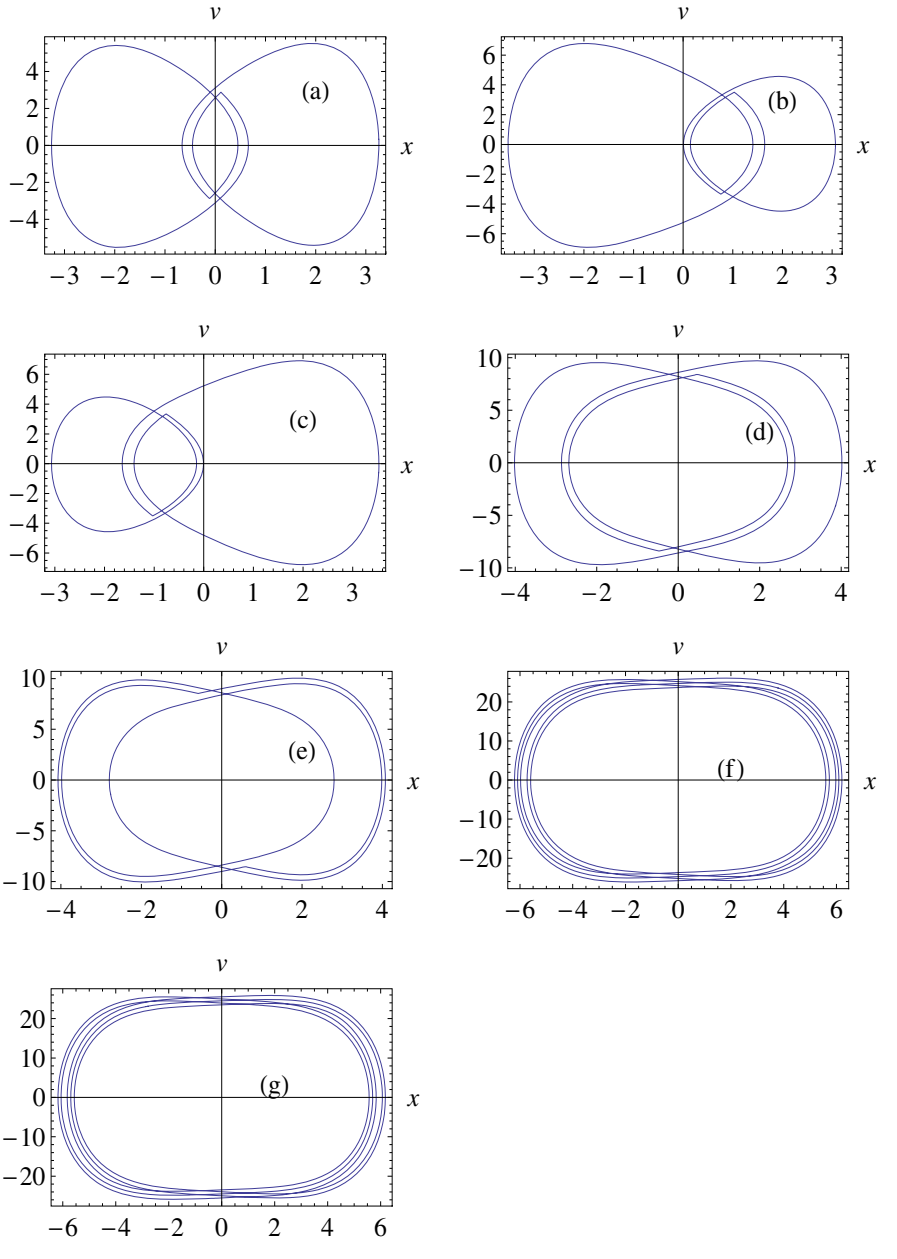

Fig. 12.7 The projections of periodic trajectories on xv-planes.

intersections are difficult to determine due to a very small angle between the intersecting curves.

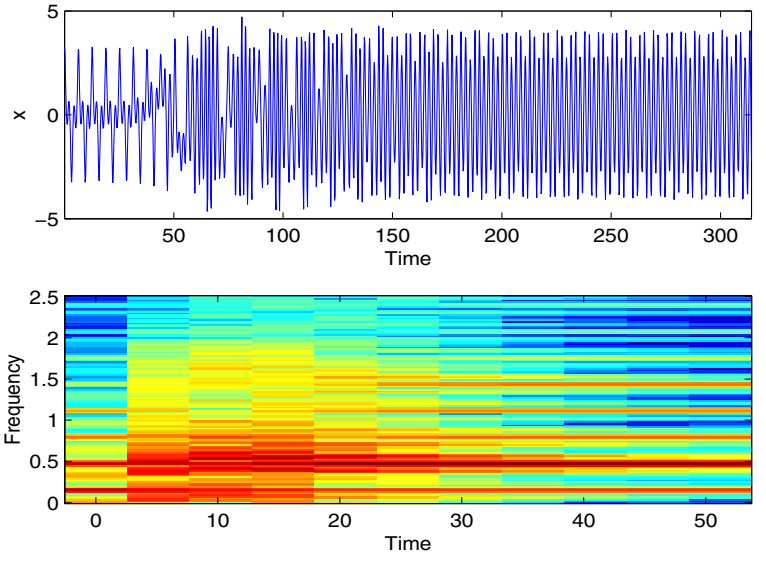

Fig. 12.8 The time history record and its spectrogram (in Hz) for evolution of the solution (a) under the step-wise voltage of the amplitude $B = 7.4$.

12.4 Other Applications

12.4.1 Periodic Solutions of the Period - n

The above sections deal with periodic solutions with the input period $T = 4a$. In order to capture 'subharmonic' solutions of the period nT, the components of representation (12.3) must be taken in the form

$$\begin{aligned} X(\tau) &= \frac{1}{2}\left[x(na\tau) + x(2na - na\tau)\right] \\ Y(\tau) &= \frac{1}{2}\left[x(na\tau) - x(2na - na\tau)\right] \end{aligned} \tag{12.39}$$

where $\tau = \tau(t/(na))$.

For instance, applying (12.39) to the sine wave $\sin \omega t$, gives

$$\begin{aligned} \sin \omega t &= \frac{1}{2}\left[\sin \frac{n\pi\tau}{2} + \sin\left(n\pi - \frac{n\pi\tau}{2}\right)\right] \\ &\quad + \frac{1}{2}\left[\sin \frac{n\pi\tau}{2} - \sin\left(n\pi - \frac{n\pi\tau}{2}\right)\right]\tau' \\ &= \frac{1}{2}\sin \frac{n\pi\tau}{2}\left\{\left[1 + (-1)^{n+1}\right] + \left[1 - (-1)^{n+1}\right]\tau'\right\} \end{aligned} \tag{12.40}$$

where $\tau' = d\tau(t/(na))/d(t/(na))$ and $a = \pi/(2\omega)$.

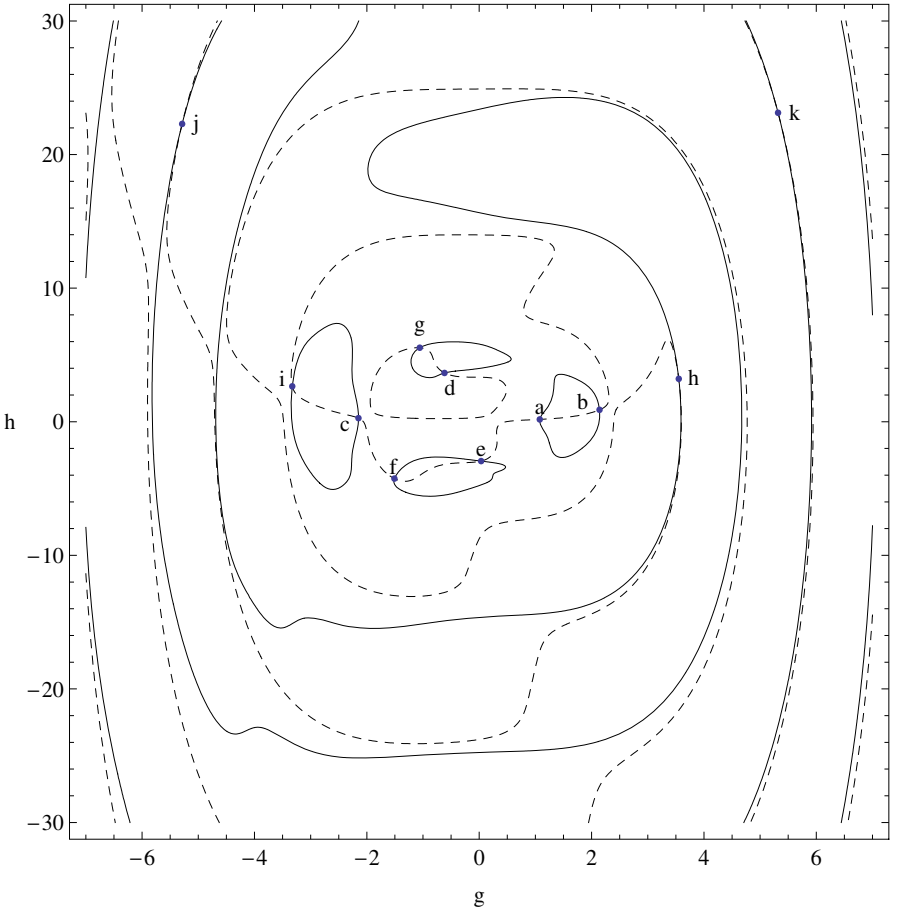

Fig. 12.9 The curves $G(g,h)=0$ (continuous) and $H(g,h)=0$ (dashed) for Ueda circuit under the impulsive input and parameters: $\zeta=0.05$, $B=1.4$, and $\omega=1$.

According to representation (12.40), equations (12.23) and (12.24) must be modified as follows

$$\begin{aligned}
&(na)^{-2}X''+\zeta(na)^{-1}Y'+X^3+3XY^2\\
&=\frac{B}{2}\left[1+(-1)^{n+1}\right]\sin\frac{n\pi\tau}{2}\\
&(na)^{-2}Y''+\zeta(na)^{-1}X'+Y^3+3X^2Y\\
&=\frac{B}{2}\left[1-(-1)^{n+1}\right]\sin\frac{n\pi\tau}{2}
\end{aligned}\tag{12.41}$$

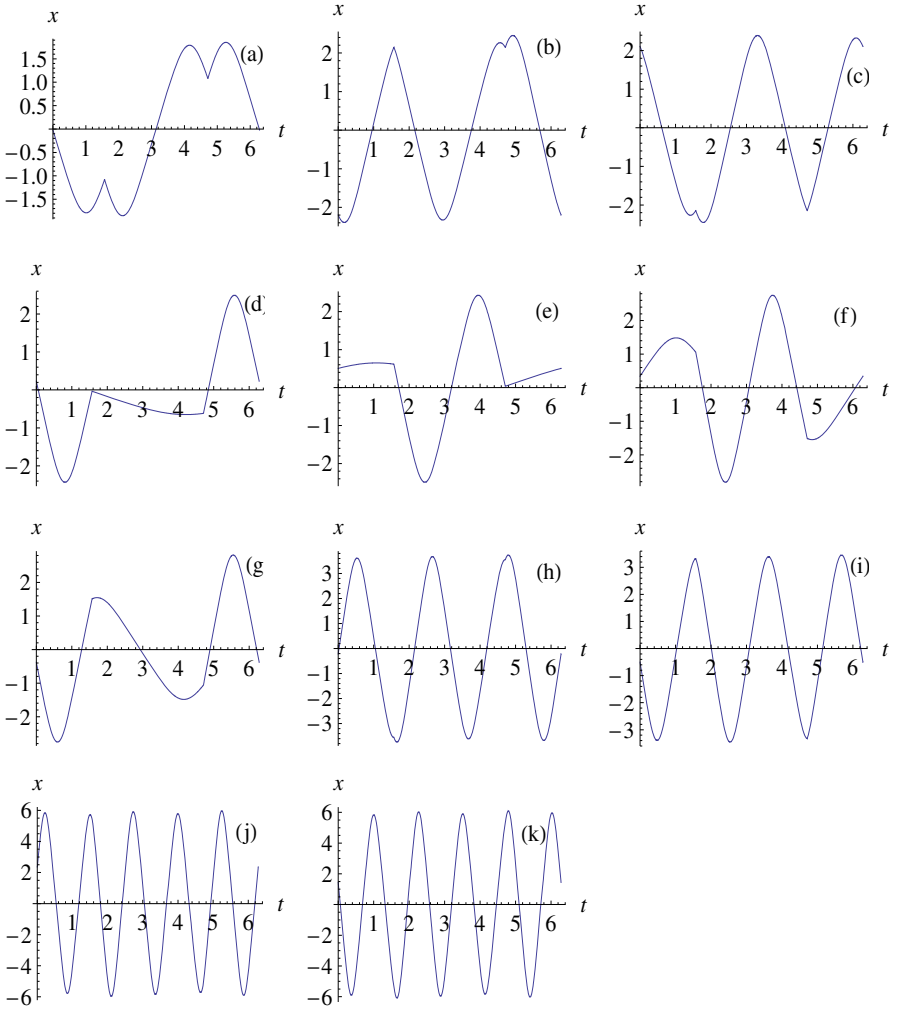

Fig. 12.10 The temporal mode shapes of periodic solutions og Ueda circuit under the impulsive input.

The right-hand side of these equations shows that direct replacement $a \to na$ in (12.23) and (12.24) would not work.

If $n = 1$ then equations (12.41) take the form (12.23) and (12.24), but if $n > 1$ equations (12.41) can give new solutions in addition to those described by equations (12.23) and (12.24). The corresponding calculations however become time consuming and give complicated diagrams as the number n increases.

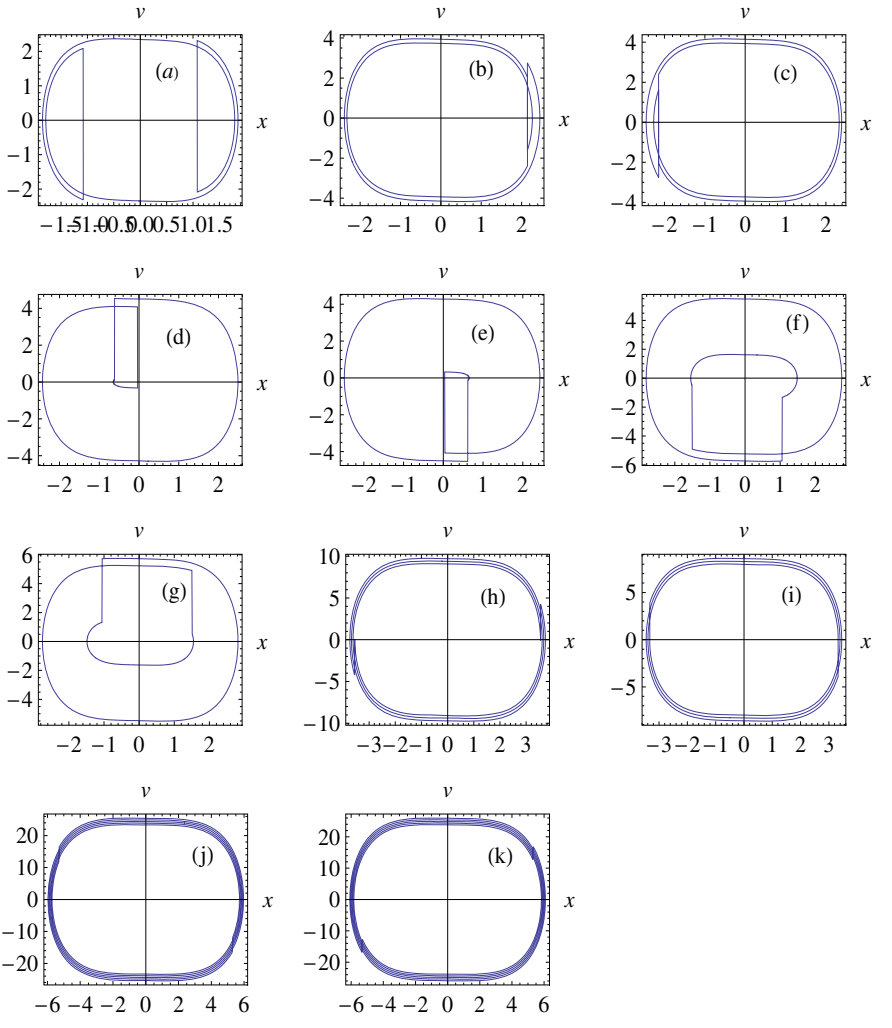

Fig. 12.11 The projections of periodic trajectories on xv-planes.

12.4.2 Two-Degrees-of-Freedom Systems

Using the above two-dimensional geometrization of shooting diagrams enables one of considering special cases of two-degrees-of-freedom systems based on equations (12.20) or (12.21). For example, equation (12.20) can be treated as an equation with respect to the two-component vector-function $X = \{X_1(\tau), X_2(\tau)\}$. Such an interpretation leads to two scalar equations

$$\begin{aligned} a^{-2}X_1'' + f_1(X_1, X_2, X_1'/a, X_2'/a, a\tau) &= Q_1(\tau) \\ a^{-2}X_2'' + f_2(X_1, X_2, X_1'/a, X_2'/a, a\tau) &= Q_2(\tau) \end{aligned} \qquad (12.42)$$

In this case, the shooting procedure should be based on the initial conditions at $\tau = -1$,

$$\begin{aligned} X_1(-1) &= g, \quad X_1'(-1) = 0 \\ X_2(-1) &= h, \quad X_2'(-1) = 0 \end{aligned} \tag{12.43}$$

where the numbers g and h are determined to satisfy the boundary conditions on the right end of the interval $-1 \leq \tau \leq 1$,

$$\begin{aligned} \frac{\partial X_1(\tau; g, h)}{\partial \tau}|_{\tau=1} &\equiv G(g, h) = 0 \\ \frac{\partial X_2(\tau; g, h)}{\partial \tau}|_{\tau=1} &\equiv H(g, h) = 0 \end{aligned} \tag{12.44}$$

In this case, every solution g and h of system (12.44) gives the initial position on the configuration plane X_1X_2 at which the system starts with zero velocity its periodic motion of the period $T = 4a$.

12.4.3 The Autonomous Case

The nonlinear normal modes represent an important class of periodic motions. The related references and description of analytical methods can be found in [100] and [190]. Analogously to the linear theory, the basic nonlinear normal mode solutions are given by the class of autonomous conservative systems. In this case, equations (12.42) take the form

$$\begin{aligned} a^{-2}X_1'' + f_1(X_1, X_2) &= 0 \\ a^{-2}X_2'' + f_2(X_1, X_2) &= 0 \end{aligned} \tag{12.45}$$

The form of equations (12.45) is easier than (12.42), but the parameter a becomes unknown. It is possible to avoid determining the parameter a by considering it as a control parameter for tracking the evolution of shooting diagrams. Alternatively, the parameter a can be considered as a shooting parameter by imposing one constraint on the parameters g or h. Let us consider, for instance, the system trajectories in the configuration plane X_1X_2. Introducing the amplitude $A = \sqrt{g^2 + h^2}$ in (12.43), gives

$$\begin{aligned} X_1(-1) &= A\cos\varphi \\ X_2(-1) &= A\sin\varphi \end{aligned}$$

where the angle φ $(0 \leq \varphi < 2\pi)$ together with the parameter a can play the role of a new unknowns to be determined by shooting whereas the amplitude A is considered as a control parameter.